Physics Letters B 811 (2020) 135854

Contents lists available at ScienceDirect

Physics Letters B

www.elsevier.com/locate/physletb

Multiphonon longitudinal wobbling in ^{127}Xe

S. Chakraborty [a,*,1], H.P. Sharma [a,*], S.S. Tiwary [a], C. Majumder [a], A.K. Gupta [a], P. Banerjee [b], S. Ganguly [c], S. Rai [d], Pragati [e], Mayank [f], S. Kumar [g], A. Kumar [h], R. Palit [i], S.S. Bhattacharjee [j], R.P. Singh [j], S. Muralithar [j]

[a] *Department of Physics, Institute of Science, Banaras Hindu University, Varanasi, India*
[b] *Nuclear Physics Division, Saha Institute of Nuclear Physics, Kolkata, India*
[c] *Department of Physics, Bethune College, Kolkata, India*
[d] *Department of Physics, Visva-Bharati, Santiniketan, India*
[e] *Department of Physics, Indian Institute of Technology, Roorkee, India*
[f] *Amity Institute of Nuclear Science and Technology, Amity University, Noida, India*
[g] *Department of Physics and Astrophysics, University of Delhi, New Delhi, India*
[h] *Department of Physics, Panjab University, Chandigarh, India*
[i] *Department of Nuclear and Atomic Physics, Tata Institute of Fundamental Research, Mumbai, India*
[j] *Nuclear Physics Group, Inter-University Accelerator Centre, New Delhi, India*

ARTICLE INFO

Article history:
Received 22 June 2020
Received in revised form 8 October 2020
Accepted 8 October 2020
Available online 15 October 2020
Editor: D.F. Geesaman

Keywords:
Longitudinal wobbling mode
Multi-phonon excitations

ABSTRACT

A family of four odd parity bands in ^{127}Xe has been investigated via in-beam γ-ray spectroscopy and conclusive evidence for the first and second phonon longitudinal wobbling excitations has been found. Spectroscopic measurements confirm the predominant $E2$ character of the $\Delta I = 1$ transitions between the wobbling bands. This provides the first experimental evidence of longitudinal wobbling mode associated with a neutron configuration.

Possibility of the wobbling motion in an *even-even* triaxially deformed nucleus was predicted first by A. Bohr and B.R. Mottelson where no intrinsic angular momentum was involved [1]. I. Hamamoto showed that the alignment of a high-j nucleon in an odd-A nucleus can drive the nucleus towards a triaxial shape and make it suitable to exhibit the wobbling motion [2]. S. Frauendorf and F. Dönau classified the wobbling mode as *longitudinal* and *transverse* in the odd-A nuclei having three axes: *l*ong, *m*edium, and *s*hort with different moments of inertia (MoI) [3]. For the longitudinal (transverse) mode, the angular momentum vector ($\boldsymbol{j}$) of the odd particle is parallel (perpendicular) to the axis with the largest MoI. In a transverse wobbler, a particle-like (hole-like) quasi-particle, emerges from the bottom (top) of a deformed j shell, aligns its $\boldsymbol{j}$ with the s-axis (l-axis). On the other hand, a triaxial nucleus becomes a longitudinal wobbler when the quasi-particle emerges from the middle of a deformed j shell and tends to align its $\boldsymbol{j}$ with the m-axis. A pictorial representation of the angular momentum geometry of different types of wobbling mode and its difference from the signature partner is available in Ref. [4]. The wobbling energy (E_{wobb}) is defined as [3]:

$$E_{\text{wobb}} = E(I, n_\omega = 1) - [E(I-1, n_\omega = 0) + E(I+1, n_\omega = 0)]/2$$

where, n_ω is the wobbling phonon number. An increasing (decreasing) trend of the E_{wobb}, as a function of angular momentum, can classify the wobbling nature as longitudinal (transverse) [3].

The wobbling mode is unique to the rotational motion of a triaxial nucleus and hence, considered as one of the fingerprints of an axially asymmetric shape of an atomic nucleus. Rotation of a triaxially deformed nucleus, having three different MoI $\mathcal{J}_x > \mathcal{J}_y \neq \mathcal{J}_z$, leads to an observation of a series of rotational $\Delta I = 2$ $E2$ bands, characterized by the wobbling phonon number, n_ω [1]. These wobbling bands with an increasing number of wobbling quanta ($n_\omega = 0, 1, 2, 3, \ldots$) are expected to have similar intrinsic structure and as a consequence, they exhibit similar rotational and more importantly electromagnetic properties [5]. Apart from the wobbling phonon number (n_ω), two successive wobbling bands are also differed by the signature quantum number (α). But, unlike signature

* Corresponding authors.
E-mail addresses: chakraborty.saikat98@gmail.com (S. Chakraborty), hpsharma_07@yahoo.com (H.P. Sharma).

[1] Present address: Nuclear Physics Group, Inter-University Accelerator Centre, New Delhi, India.

https://doi.org/10.1016/j.physletb.2020.135854
0370-2693/

partner bands, collectively enhanced $\Delta I = 1$ $E2$ transitions are expected to be observed between these consecutive wobbling bands. Therefore, it is important to decompose the $E2$ and $M1$ amplitudes of the observed γ-rays between the wobbling bands with $\Delta n_\omega = 1$. A large value of $B(E2)_{out}/B(E2)_{in}$ of $\Delta I = 1\hbar$ interband to $\Delta I = 2\hbar$ intraband $E2$ transitions can serve as evidence of wobbling motion in nuclei [6].

Experimentally, the wobbling motion was first realised in $A \approx 160$ region, namely, in ^{163}Lu [7], followed by ^{161,165,167}Lu [8–10] and ^{167}Ta [11] nuclei. In the cases of ^{163,165}Lu, the second-phonon wobbling excitation was also reported [6,9]. These wobbling bands were associated with $\pi i_{13/2}$ configuration and tri-axially strongly deformed ($\epsilon \approx 0.4$) in nature [3,12]. Possibility of wobbling motion in $A \approx 130$ region with lesser deformation ($\epsilon \approx 0.16$) was also predicted in ^{135}Pr [3] and subsequently observed experimentally [13]. Later, the second-phonon wobbling band was also identified in this nucleus [14]. Apart from the ^{135}Pr, the ^{133}La [15] is also reported to exhibit wobbling motion in this mass region. Recently, presence of the wobbling band was also confirmed in ^{105}Pd [16] and ^{183,187}Au [4,17], outside of the $A \approx 130$ region. In the context of the wobbling mode in odd-A nuclei, it is worth noting that, the wobbling motion in all the nuclei, apart from the ^{133}La and ^{187}Au, is transverse in nature and associated with a one-quasiproton configuration, except in the case of ^{105}Pd.

Over the past few decades, a lot of attention has been paid to the structure of the negative parity bands in the odd-A Xe nuclei because of the anomaly in observed signature splitting. The yrast bands, originating due to the coupling of an $h_{11/2}$ quasineutron to the ground state configuration of the even-even core, were reported with a large signature splitting, S(I), in spite of having high-Ω configurations ($\Omega \geq \frac{5}{2}$) [18–25]. Interestingly, the so-called unfavoured signature partner of $\pi h_{11/2}$ band (after some rearrangement) in ^{135}Pr has been reinterpreted recently in terms of wobbling excitation [13,26]. Following this, the unfavoured signature partner of $\pi h_{11/2}$ ($\pi h_{9/2}$) band in ^{133}La (^{187}Au) has also been revisited and evidence for its wobbling nature has been found [4,15,27,28]. In contrast to the large S(I) in the yrast bands, the yrare bands were reported with a low, fairly constant and inverted signature splitting [25,29–31]. The origin of these yrare bands is thought to be due to the coupling of an $h_{11/2}$ neutron with the γ-vibration of the core [31]. But, the S(I) of the quasi-γ-bands in the core is not inverted and also varies with the mass number [32]. Therefore, the origin of the yrare bands is not fully understood and demands further investigation. In this work, an attempt has been made to infer the structure of the negative parity bands in ^{127}Xe.

Excited states of ^{127}Xe were populated by the bombardment of 48 MeV ^{9}Be beam, delivered by the 15UD pelletron accelerator [33] of Inter-University Accelerator Centre (IUAC), New Delhi, on an 8.4 mg/cm^2 thick 99.3% isotopically enriched ^{122}Sn target [34]. At this beam energy, the 4n evaporation channel is found to be the most dominant with more than 50% of the total fusion-evaporation reaction cross-section [34]. The INGA [35] spectrometer, consisting of fourteen Compton suppressed HPGe clover detectors, was used to collect $\approx 9 \times 10^8$ two and higher fold coincident γ-events which were recorded by CANDLE [36] data acquisition software. Offline data analysis was carried out using codes INGASORT [37] and RADWARE [38]. Details of the experimental set-up and data analysis procedures are available in the earlier publications from the same experiment [39–41].

A partial level scheme of ^{127}Xe deduced from this work is shown in Fig. 1. The levels are grouped into bands 1-4 based on the $\gamma\gamma$-coincidence and intensity relationship. Pertinent energy gated γ-spectra are shown in Fig. 2 in support of the placement of new γ-transitions in the level scheme. Detailed spectroscopic results are given in the Supplementary Material [42]. Apart from the negative parity bands shown in Fig. 1, several other positive parity bands were also observed in this nucleus [43–46]. The full level scheme of ^{127}Xe is available in Ref. [47] and will be presented in a forthcoming publication.

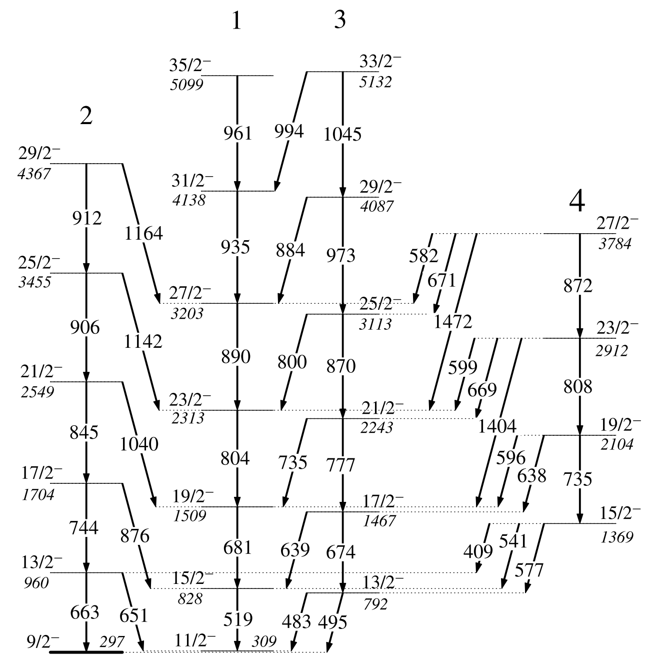

Fig. 1. Partial negative parity level scheme of ^{127}Xe.

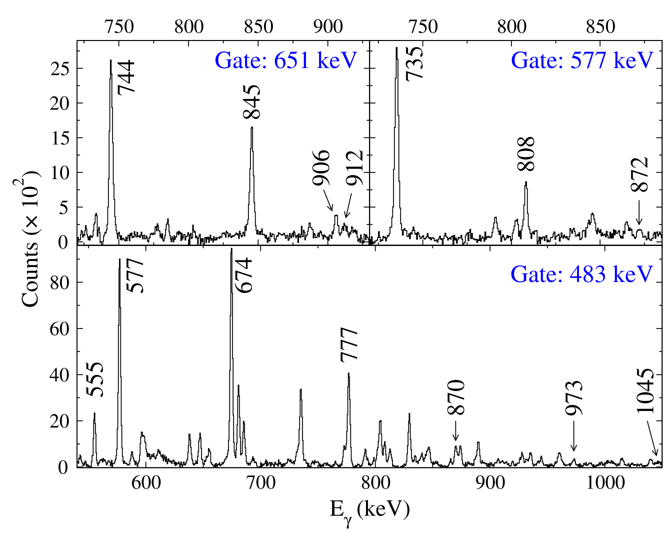

Fig. 2. Prompt γ-rays observed in coincidence with 651, 577 and 483 keV γ-rays belonging to bands 2-4 in ^{127}Xe. Transitions of present interest are marked in keV.

Band 1 is a negative parity sequence which was reported earlier up to $I^\pi = (51/2^-)$ [39,48]. No new γ-ray belonging to this band is identified in this work. Previously, band 2 was reported up to $I^\pi = (17/2)^-$ at 1704 keV [22,45]. In this work, three additional γ-transitions, *viz.* $E_\gamma = 845, 906, 912$ keV (Fig. 2), have been placed in this band to extend it up to $I^\pi = 29/2^-$ at 4367 keV. Band 3, reported earlier up to $I^\pi = 21/2^-$ at 2243 keV [22,43], has also been extended in this work up to $I^\pi = 33/2^-$ at 5132 keV by the addition of $E_\gamma = 870, 973, 1045$ keV γ-transitions (Fig. 2). Another cascade of three γ-transitions, *viz.* $E_\gamma = 735, 808, 872$ keV (Fig. 2), have been established above $I^\pi = 15/2^-$ state at 1369 keV. First two energy levels of this band were reported earlier [22]. Placement of two more new γ-transitions in this work leads to an extension of this band up to $I^\pi = 27/2^-$ state at 3784 keV. All the energy levels of bands 2 and 3 have been found to decay into

Table 1
List of the experimental DCO ratio (R_{DCO}), linear polarization asymmetry (Δ_{asym}), multipole mixing ratio ($\delta_{E2/M1}$), $E2$ fraction and the transition probability ratios for some $\Delta I = 1$ inter-band γ-transitions belonging to ^{127}Xe.

E_γ (keV)	$I_i^\pi \to I_f^\pi$ ($\hbar$)	R_{DCO} (err)	Δ_{asym} (err)	$\delta_{E2/M1}$ (err)	$E2$ fraction (%)	$\frac{B(M1)_{out}}{B(E2)_{in}}$ $(\frac{\mu_N^2}{e^2b^2})$	$\frac{B(E2)_{out}}{B(E2)_{in}}$
483	$13/2^- \to 11/2^-$	0.303 (21)	+0.058 (32)	$-2.1^{+0.2}_{-0.2}$	$81.5^{+2.6}_{-3.2}$		
639	$17/2^- \to 15/2^-$	0.304 (15)	+0.008 (36)	$-2.2^{+0.2}_{-0.1}$	$82.9^{+2.3}_{-1.4}$	0.138 (12)	2.352 (565)
735	$21/2^- \to 19/2^-$	0.313 (10)	+0.031 (25)	$-2.4^{+0.1}_{-0.1}$	$85.2^{+1.0}_{-1.1}$	0.098 (5)	1.500 (172)
800	$25/2^- \to 23/2^-$	0.352 (41)	+0.074 (61)	$-2.9^{+0.7}_{-0.5}$	$89.4^{+3.5}_{-4.2}$	0.071 (31)	1.346 (879)
884	$29/2^- \to 27/2^-$	0.366 (88)	+0.048 (82)	$-3.1^{+1.9}_{-1.1}$	$90.6^{+5.6}_{-10.6}$	0.052 (44)	0.922 (895)
577	$15/2^- \to 13/2^-$	0.245 (28)	+0.051 (37)	$-1.7^{+0.2}_{-0.3}$	$74.3^{+4.0}_{-8.1}$		
638	$19/2^- \to 17/2^-$	0.311 (66)	+0.068 (115)	$-2.4^{+0.9}_{-0.7}$	$85.2^{+6.4}_{-10.9}$	0.062 (26)	1.364 (999)
651	$13/2^- \to 11/2^-$	0.717 (69)	−0.012 (137)	$+0.15^{+0.05}_{-0.05}$	$2.2^{+1.6}_{-1.3}$	0.180 (4)	0.014 (9)
876	$17/2^- \to 15/2^-$	0.849 (132)	−0.114 (132)	$+0.26^{+0.10}_{-0.10}$	$6.5^{+5.4}_{-3.9}$	0.053 (2)	0.007 (5)

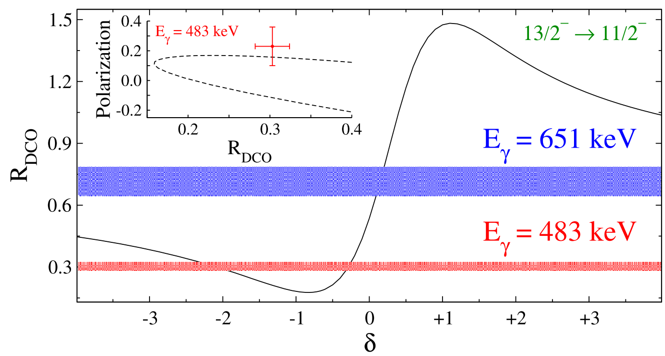

Fig. 3. Variation of theoretical DCO ratio (black line) as a function of the mixing ratio (δ) for the $13/2^- \to 11/2^-$ ($\Delta I = 1$) γ-ray. The $17/2^- \to 13/2^-$ ($\Delta I = 2$) transition was considered as the gate. The red (blue) shaded region corresponds to the experimental R_{DCO} of 483 (651) keV γ-ray. Inset: Experimental data (red dot) and theoretical contour plot (black dashed line) of DCO Ratio versus linear polarization, as a function of δ, for 483 keV γ-ray.

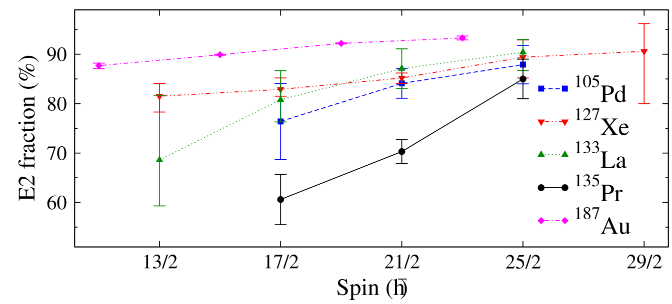

Fig. 4. Plot of $E2$ admixture, as a function of spin, in the $\Delta I = 1$ γ-rays between $n_\omega = 1$ and $n_\omega = 0$ wobbling bands in different nuclei at low spin regime.

band 1 by $\Delta I = 1$ γ-transitions. However, the states belonging to band 4 have been found to decay into both band 1 and band 3 via $\Delta I = 0, 1, 2$ γ-transitions.

Spin and parity of these states have been assigned based on the results of angular correlation and linear polarization measurements [42]. The $E2/M1$ multipole mixing ratio (δ) of some $\Delta I = 1$ inter-band γ-transitions has been estimated by comparing the experimental DCO ratio with the corresponding theoretical values, calculated for the different values of δ, using the computer code ANGCOR [49], as shown in Fig. 3 for $E_\gamma = 483$ and 651 keV γ-transitions. The present analysis resulted in a mixing ratio of $\delta = -2.1^{+0.2}_{-0.2}$ or $-0.29^{+0.03}_{-0.04}$ for the 483 keV lowest inter-band $\Delta I = 1$ transition between band 1 and band 3. This agrees well with the earlier reported result of $\delta = -1.7^{+0.4}_{-0.6}$ or $-0.45^{+0.12}_{-0.12}$, determined from the angular distribution studies [22]. However, the linear polarization (P = 0.23 (13) [this work] or 0.22 (3) [22]) of 483 keV γ-transition supports the higher magnitude of δ as shown in the inset of Fig. 3. Therefore, the presence of a high $E2$ admixture in 483 keV γ-transition is concluded. The present value of $\delta = +0.15^{+0.05}_{-0.05}$ for the 651 keV lowest inter-band $\Delta I = 1$ transition between band 1 and band 2 agrees only within the error limits with the earlier result of $\delta = +0.03^{+0.07}_{-0.07}$ [22]. Good data statistics permit the assignment of lower error limits in the present δ value. In contrast to the case of 483 keV γ-ray, the present R_{DCO} of 651 keV γ-transition indicates only one value of δ within $-4 \le \delta \le +4$ limit. Another larger value of $\delta = +30^{+\infty}_{-20}$ was also reported for this transition, which indicates $\approx 99.9\%$ $E2$ content [22]. The linear polarization (P = −0.4 (3) [22]), although having a large error bar, disagree with such a high mixing ratio. Present linear polarization asymmetry of the 651 keV γ-ray contains large uncertainty mainly due to the poor population of band 2. Moreover, the presence of a contaminant 652 keV $E2$ γ-transition in coincidence with 745 keV $E2$ γ-transition in neighbouring ^{127}I nucleus also influence the magnitude of the linear polarization asymmetry [50]. Nevertheless, the R_{DCO} = 0.61 (4) of 486 keV $E1$ γ-transition in ^{127}Xe [43], R_{DCO} = 0.62 (3)/0.61 (5)/0.66 (8) of 490/215/254 keV $E1/M1/M1$ γ-transitions in ^{127}I [51] and R_{DCO} = 0.61 (5) of 718 keV $E1$ γ-transition in ^{125}Te [41] was also found quite similar to that of 651 keV transition and hence, support the smaller δ value. Spectroscopic results of some of the important $\Delta I = 1$ γ-transitions are summarized in Table 1.

The $\Delta I = 2$ negative parity rotational bands, as shown in Fig. 1, were also observed in lighter ^{odd}Xe isotopes and identified as the yrast (marked as band 1 and band 3 in Fig. 1) and yrare (marked as band 2 and band 4 in Fig. 1) bands based on $\nu h_{11/2}$ orbital [25,29–31]. Theoretical calculation predicts that the signature splitting in yrast bands is very sensitive to the γ-deformation [52]. For instance, the observed S(I) in the case of ^{125}Xe ($[523]\frac{7}{2}$) is reproduced well with $\gamma \approx 24°$ [53]. However, the non-yrast nature of the unfavoured signature partner of $\pi h_{11/2}$ band in ^{135}Pr was predicted from QTR calculation [13]. In this scenario, it becomes important to identify the proper signature partner of the $\nu h_{11/2}$ band in ^{127}Xe. As per the spin-parity assignment and the decay pattern of the γ-rays, both band 2 and band 3 are the potential candidates for the unfavoured signature partner of band 1. Normally, however, in the case of signature partner bands, the $\Delta I = 1$ inter-band γ-rays are expected to be predominantly $M1$ in nature. Therefore, band 2, rather than band 3, is the right choice for the unfavoured signature partner of band 1.

The $\Delta I = 1$ inter-band transitions between band 1 and band 3 have predominantly $E2$ character. Existence of such highly mixed γ-transitions between two quadrupole bands is a unique signature of wobbling excitation in an atomic nucleus [7]. The $E2$ fractions of these inter-band transitions are found to increase further with increasing angular momentum (Fig. 4). This feature is also observed

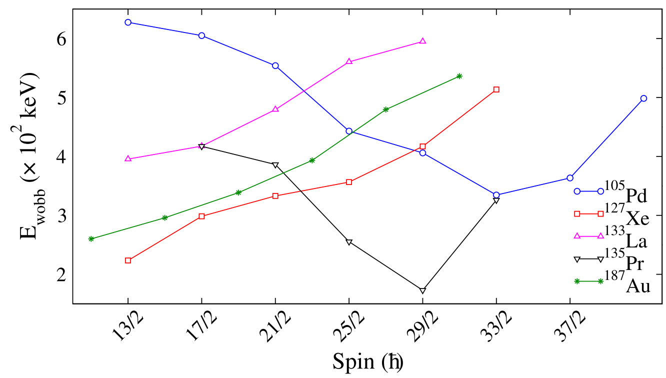

Fig. 5. Variation of wobbling energies with spin for the $n_\omega = 0, 1$ wobbling bands pair in ^{105}Pd [16], ^{133}La [15], ^{135}Pr [13], ^{187}Au [4] and ^{127}Xe [this work].

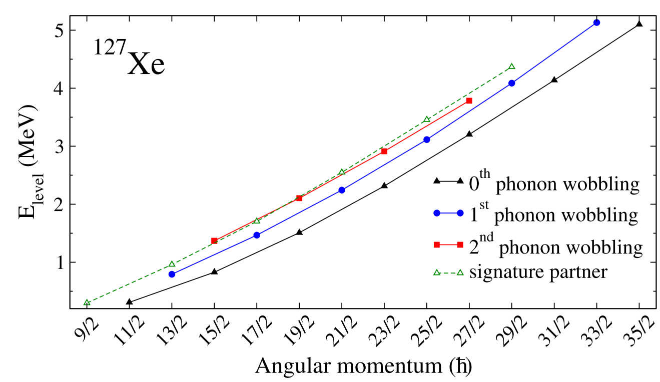

Fig. 6. Plot of level energies of the negative parity bands as a function of angular momentum (I).

in other cases of wobbling excitations reported in the low spin regime [4,13,15,16]. The $B(M1)_{out}/B(E2)_{in}$ and $B(E2)_{out}/B(E2)_{in}$ transition probability ratios, listed in Table 1, for these $\Delta I = 1$ transitions are also found to be similar to those reported in the cases of other wobbling excitations [42]. Therefore, the origin of band 3 can be explained in terms of the first phonon wobbling excitation ($n_\omega = 1$) in this nucleus. The energy of the $n_\omega = 1$ band 3 relative to the $n_\omega = 0$ band 1 is known as the wobbling energy (E_{wobb}). Fig. 5 represents the plot of E_{wobb} as a function of angular momentum for different wobbling bands reported in the low spin regime. The wobbling energy for ^{127}Xe shows an increasing trend with spin similar to that of ^{133}La and ^{187}Au. This suggests the existence of longitudinal wobbling mode in this nucleus. The first phonon wobbling band is found lower in excitation energy than the unfavoured signature partner band (Fig. 6), as was predicted in the case of ^{135}Pr [13]. Non-yrast nature of the unfavoured signature partner band is possibly responsible for its lesser population in ^{127}Xe.

The $\Delta I = 1$ inter-band transitions between band 3 and band 4 also have large $E2$ admixtures. The energy levels of this band are found to decay into both band 1 and band 3 through $\Delta I = 2, 1$ γ-transitions, respectively. Earlier, similar kind of decay pattern and/or transition probability ratios were observed in the case of second phonon transverse wobbling band in ^{163,165}Lu [6,9] and ^{135}Pr [14]. Thus, this band possibly originates due to the second phonon longitudinal wobbling excitation. This provides the first experimental evidence of second phonon longitudinal wobbling mode in an atomic nucleus. Interestingly, all the energy levels of band 4 ($n_\omega = 2$) are also found to decay into band 1 ($n_\omega = 0$) via $\Delta I = 0$ transitions. These $\Delta I = 0$ transitions are found to be more intense than the $\Delta I = 2$ transitions between the same two bands 1 and 4. However, no such $\Delta I = 0$ transitions between the $n_\omega = 2$ and $n_\omega = 0$ wobbling bands were observed in the previous three cases of two-phonon bands. Rather, this decay pattern is quite similar to that observed between the ground state band and the even spin sequence of the quasi-γ band in ^{126}Xe [32]. Therefore, it might be an indication of the coupling between wobbling motion and γ-vibration in this nucleus. Such type of coupling was also predicted in ^{164}Hf using self-consistent calculations based on the tilted-axis cranking model [54]. A further theoretical investigation is essential to infer the microscopic structure of this band in ^{127}Xe.

Thus, the present study can successfully address the long-standing issue on the structure of negative parity bands in odd-A Xe nuclei. The configuration of the observed negative parity bands in ^{127}Xe can be summarised as follows in term of wobbling excitation:

Band 1: $n_\omega = 0$ wobbling band ($\alpha = -\frac{1}{2}$),
Band 2: $n_\omega = 0$ wobbling band ($\alpha = +\frac{1}{2}$),
Band 3: $n_\omega = 1$ wobbling band, and
Band 4: $n_\omega = 2$ wobbling band.

To conclude, the ^{127}Xe has been identified as the third nucleus to exhibit longitudinal wobbling excitation. This Letter reports the first observation of longitudinal wobbling mode in a nucleus with an odd-neutron. The second phonon longitudinal wobbling band is also observed in this work for the first time in an atomic nucleus.

Declaration of competing interest

The authors declare that they have no known competing financial interests or personal relationships that could have appeared to influence the work reported in this paper.

Acknowledgement

Authors are thankful to the staff of the target lab and pelletron accelerator of IUAC, New Delhi. The effort from INGA collaboration, partly funded by the University Grants Commission (UGC) and Department of Science and Technology (DST), Government of India (INGA project no. IR/S2/PF-03/2003-I), to make the detectors available and set the array at IUAC is thankfully acknowledged. SC is also thankful to the Council of Scientific & Industrial Research (CSIR), India, for Senior Research Fellowship *vide* file no. 9/13(662)/2017-EMR-I and to the Inter-University Accelerator Centre (IUAC), New Delhi for Research Associateship *vide* ref. no. IUAC/SC/RA/2019/5290.

Appendix A. Supplementary material

Supplementary material related to this article can be found online at https://doi.org/10.1016/j.physletb.2020.135854.

References

[1] A. Bohr, B.R. Mottelson, Nuclear Structure, Vol. II, Benjamin, New York, 1975.
[2] I. Hamamoto, Phys. Rev. C 65 (2002) 044305.
[3] S. Frauendorf, F. Dönau, Phys. Rev. C 89 (2014) 014322.
[4] N. Sensharma, et al., Phys. Rev. Lett. 124 (2020) 052501.
[5] G.B. Hagemann, Acta Phys. Pol. B 36 (2005) 1043.
[6] D.R. Jensen, et al., Phys. Rev. Lett. 89 (2002) 142503.
[7] S.W. Ødegård, et al., Phys. Rev. Lett. 86 (2001) 5866.
[8] P. Bringel, et al., Eur. Phys. J. A 24 (2005) 167.
[9] G. Schönwaßer, et al., Phys. Lett. B 552 (2003) 9.
[10] H. Amro, et al., Phys. Lett. B 553 (2003) 197.
[11] D.J. Hartley, et al., Phys. Rev. C 80 (2009) 041304.
[12] G.B. Hagemann, Eur. Phys. J. A 20 (2004) 183.
[13] J.T. Matta, et al., Phys. Rev. Lett. 114 (2015) 082501.
[14] N. Sensharma, et al., Phys. Lett. B 792 (2019) 170.
[15] S. Biswas, et al., Eur. Phys. J. A 55 (2019) 159.
[16] J. Timár, et al., Phys. Rev. Lett. 122 (2019) 062501.
[17] S. Nandi, et al., Phys. Rev. Lett. 125 (2020) 132501.

[18] Z. Liu, et al., Eur. Phys. J. A 1 (1998) 125.
[19] J. Timár, et al., J. Phys. G 21 (1995) 783.
[20] A. Basu, et al., Phys. Rev. C 101 (2020) 024309.
[21] A. Al-Khatib, et al., Phys. Rev. C 83 (2011) 024306.
[22] W. Urban, et al., Z. Phys. A 320 (1985) 327.
[23] Y. Huang, et al., Phys. Rev. C 93 (2016) 064315.
[24] R. Banik, et al., Phys. Rev. C 101 (2020) 044306.
[25] C.-B. Moon, et al., Eur. Phys. J. A 14 (2002) 13.
[26] T.M. Semkow, et al., Phys. Rev. C 34 (1986) 523.
[27] C.M. Petrache, et al., Phys. Rev. C 94 (2016) 064309.
[28] J.K. Johansson, et al., Phys. Rev. C 40 (1989) 132.
[29] C.-B. Moon, et al., Eur. Phys. J. A 4 (1999) 107.
[30] A. Gade, et al., Nucl. Phys. A 686 (2001) 3.
[31] C.-B. Moon, et al., Phys. Rev. C 76 (2007) 067301.
[32] S. Chakraborty, et al., Nucl. Phys. A 996 (2020) 121687.
[33] G.K. Mehta, A.P. Patro, Nucl. Instrum. Methods Phys. Res., Sect. A 268 (1988) 334.
[34] S. Chakraborty, et al., Phys. Scr. 93 (2018) 115302.
[35] S. Muralithar, et al., Nucl. Instrum. Methods Phys. Res., Sect. A 622 (2010) 281.
[36] B.P. Ajith-Kumar, et al., in: Proc. DAE, in: Symp. Nucl. Phys., vol. 44B, 2001, p. 390.
[37] R. Bhowmik, et al., in: Proc. DAE, in: Symp. Nucl. Phys., vol. 44B, 2001, p. 422.
[38] D.C. Radford, Nucl. Instrum. Methods Phys. Res., Sect. A 361 (1995) 297.
[39] S. Chakraborty, et al., Braz. J. Phys. 47 (2017) 406.
[40] S.S. Tiwary, et al., Eur. Phys. J. A 55 (2019) 163.
[41] S. Chakraborty, et al., Europhys. Lett. 125 (2019) 52001.
[42] See Supplementary Material for detailed spectroscopic results.
[43] S. Chakraborty, et al., Phys. Rev. C 97 (2018) 054311.
[44] S. Chakraborty, et al., Eur. Phys. J. A 56 (2020) 50.
[45] S. Chakraborty, et al., J. Phys. G, Nucl. Part. Phys. 47 (2020) 015103.
[46] S. Chakraborty, et al., Europhys. Lett. 121 (2018) 42001.
[47] S. Chakraborty, Ph.D. thesis, Banaras Hindu University, Varanasi, India, 2019.
[48] I. Wiedenhöver, et al., Z. Phys. A 347 (1993) 71.
[49] E. Macias, et al., Comput. Phys. Commun. 11 (1976) 75.
[50] S. Chakraborty, et al., Eur. Phys. J. A 54 (2018) 112.
[51] S. Chakraborty, et al., J. Phys. G, Nucl. Part. Phys. 47 (2020) 095104.
[52] A. Gelberg, et al., Nucl. Phys. A 557 (1993) 439c.
[53] D. Lieberz, et al., Phys. Lett. B 282 (1992) 7.
[54] M. Oi, P.M. Walker, arXiv:nucl-th/0107051, 2001.